

Chapter 15

Geosynthetics in Retaining Walls Subjected to Seismic Shaking



G. Madhavi Latha , A. Murali Krishna, G. S. Manju,
and P. Santhana Kumar

15.1 Introduction

Usage of synthetic materials has gained a high level of confidence with the civil engineering community, after years of research and successful installations during the past half century. Constrained infrastructure budgets and rise in environmental concerns about the depleting natural construction materials have necessitated and popularized the use of synthetics in lieu of traditional construction materials in various geotechnical structures like foundations, pavements, retaining walls, embankments and engineered slopes. Special polymeric products called geosynthetics have been developed specifically to serve various functions like separation, filtration, drainage, reinforcement, containment and erosion control in variety of civil engineering applications. Reinforcing the soils with geosynthetics to improve its strength and mechanical properties has gained wide acceptance worldwide, and this technique is adopted to increase the bearing capacity of foundations, improving the stability of slopes and embankments and build vertical walls of greater heights (Koerner 2012; Chen et al. 2007; Li and Rowe 2008). Common types of geosynthetics used for soil reinforcement in retaining walls are—geotextiles, geogrids and geocells.

Under static loading conditions, role of tensile reinforcement in geotechnical structures is to provide additional confinement to the soil, which can be realized as apparent cohesion, providing additional stability against failures. During earthquake, the soil element under constant overburden pressure is subjected to cyclic simple shear stresses with alternating positive and negative values in addition to the vertical and horizontal normal stresses. These earthquake-induced shear stresses increase the difference in principal stresses, thus enlarging the Mohr circle to bring the soil element close to a failure state (Ling et al. 2009). If the induced shear

G. Madhavi Latha (✉) · A. Murali Krishna · G. S. Manju · P. Santhana Kumar
Indian Institute of Science, Bangalore 560012, India
e-mail: madhavi@iisc.ac.in

stresses are very high, the minor principal stress can be negative, thus inducing tension in soil. Since structures like retaining walls are usually built with granular soils, which cannot sustain any tension, ground surface cracks develop. Cyclic rotation of principal stress directions also occurs under seismic loading conditions, which can significantly reduce the shear strength of soils, causing further instabilities. The tensile reinforcement offers restraint to the shear deformations in soil induced by seismic events. The use of tensile reinforcement for improving the seismic stability of retaining walls has gained considerable attention in recent times and has become a very common practice.

Seismic vibrations can induce instability in otherwise stable slopes. Seismic vibrations break the contacts between soil grains and also impose additional driving forces on the slopes, thus triggering failure in cases where the shear strength of the soils is exceeded by these driving forces. Reinforced soil slopes provide better resistance to the seismic forces and possess higher yield accelerations compared to unreinforced slopes. Experiences from recent earthquake records all over the world suggest that reinforced slopes perform better during earthquakes and in many cases the unreinforced failed slopes are rebuilt using reinforcement. The confinement effect generated by the layers of reinforcement in a reinforced slope prevents the vibrations to easily transmit through soil layers unlike in the case of unreinforced slope and hence improves the stability to a great extent. Generally, geosynthetic-reinforced soil slopes are more ductile and flexible and hence more tolerant to seismic loading conditions (Leshchinsky et al. 2009).

Shaking table model studies are widely popular among geotechnical engineers to study the seismic performance of soil structures. Several earlier researchers have used shaking tables to study the seismic performance of soil structures. Shaking table tests are *1-g* model tests with the limitations of stress dissimilarities between the model and the prototype. The larger size of *1-g* shaking table tests makes it easier to use a larger number and wider range of instruments to record deformations and accelerations. Major disadvantages of shaking table modeling are the low confining pressure applied to stress-dependent backfill and reinforcement layers and the requirement to properly scale the reinforcement stiffness (El-Emam and Bathurst 2004). Rigid shaking table model containers can have undesirable influences of reflecting energy boundaries (Coe et al. 1985), which can be overcome by using laminar or shear boxes that reduce these boundary effects (Wood et al. 2002; Turan et al. 2009; Krishna and Latha 2009).

From early 1980s, many studies were reported in the literature on the use of shaking tables to understand the seismic response of reinforced retaining walls (Sakaguchi 1996; Bathurst and Hatami 1998; Perez and Holtz 2004; El-Emam and Bathurst 2007; Lo Grasso et al. 2005; Krishna and Latha 2007; Panah et al. 2015; Latha and Santhanakumar 2015; Wang et al. 2015). Height of the models was 1 m or less in majority of these studies. Most of these studies brought out the advantages of reinforced retaining walls over unreinforced walls under earthquake conditions. Since shaking table studies are *1-g* model tests, direct extrapolation of the test results to the field structures is not possible. Several researchers in the past

attempted to develop similitude laws for shaking table test results in order to apply the results to field situations (Wood et al. 2002; Clough and Pirtz 1956; Iai 1989; Sugimoto et al. 1994; Telekes et al. 1994).

Beneficial effects of soil reinforcement using geosynthetics for various types of retaining walls under different earthquake loading conditions are demonstrated in this study through shaking table model studies. Models of wrap-faced, rigid-faced and segmental retaining walls were built in a laminar box mounted on a uniaxial shaking table. These models were tested at sinusoidal earthquake loading conditions of different acceleration amplitudes and frequencies. Results from the model tests are analyzed to understand the effects of reinforcement on acceleration amplifications and deformations of the soil structures.

15.2 Shaking Table and Instrumentation

A shaking table with uniaxial degree of freedom was used for simulating earthquake motion in this study. The table is square in plan with 1 m sides and can carry a load of 10 kN. The table can be operated at an acceleration range of 0.05–2 g and frequency range of 1–50 Hz. Natural frequency of the shaking table is 100 Hz, which is much higher than the operating frequency, to make sure that the table is not subjected to resonance during model testing. A rectangular laminar box with clear inner dimensions of 1 m length, 0.5 m width and 0.8 m height was fabricated using a steel outer frame and 15 hollow aluminum panels stacked on each other with frictionless roller bearings. These bearings allow the aluminum panels to move independently during the movement of model, thus reducing the boundary effects on models. During testing, accelerations were measured using piezo-electric-type accelerometers and non-contact ultrasonic displacement transducers (USDT). Sensitivity of accelerometers is 0.001 g within the bandwidth of 1 Hz–2 kHz. The displacement sensors have response time of 30 ms and sensitivity of 0.01 mm.

15.3 Model Studies on Retaining Walls

Four different types of retaining walls, namely wrap-faced, rigid-faced, segmental and geocell walls were built inside the laminar box. Results from shaking table studies on these models are discussed in following subsections. All retaining wall models were built using poorly graded dry sand. The maximum and minimum dry unit weights of sand are 18 and 14 kN/m³, respectively. Friction angle measured from direct shear test at 65% relative density was 45°. Sand pluviation technique was used for backfilling, achieving a relative density of 65%.

15.3.1 Wrap-Faced Walls

Wrap-faced retaining walls are the retaining walls where the geotextile reinforcement itself is extended as the facing for the wall. A polypropylene multifilament-type woven geotextile was used to build these walls. The geotextile has ultimate tensile strength of 55 kN/m at peak strain of 38%, measured in wide-width tension test conducted at 10% strain rate. At low strain level (2%), the geotextile has mobilized a tensile strength of 3 kN/m, exhibiting a secant modulus of 152 kN/m. Models of wrap-faced retaining walls were of 0.75 m length oriented in the direction of horizontal shaking, 0.5 m width perpendicular to the direction of shaking and 0.6 m height. Walls were constructed in 4 lifts, each of 0.15 m thickness. Models were instrumented with accelerometers (A) and pressure transducers (P) at different locations, and three displacement transducers (U) were fixed to a rigid steel bracket connected to the laminar box frame at a distance from the retaining wall facing, as shown in Fig. 15.1. A surcharge pressure of 0.5 kPa is applied over the constructed retaining wall.

Retaining wall models were built with different lengths of reinforcement (L_{rein}) and were subjected to 20 cycles of horizontal shaking of acceleration amplitude 0.2 g and frequency 3 Hz. Reinforcement lengths of 420, 300 and 600 mm were adopted in the tests WT17, WT19 and WT20, respectively, with the corresponding normalized reinforcement length (L_{rein}/H), where H is the height of the wall, as 0.7, 0.5 and 1.0. Results from these three tests are analyzed to understand the effect of reinforcement length on facing deformations and acceleration amplifications of the wall at different elevations. Acceleration amplifications are converted to root mean square acceleration (RMSA) amplification factors so that the entire acceleration time history for each accelerometer device is integrated over the entire duration with positive and negative acceleration measurements squared and averaged over the duration to get one absolute value.

Figure 15.2 shows the displaced profiles for the test walls WT17, WT19 and WT20 with different reinforcement lengths (L_{rein}). Displacements reduced considerably with the increase in the length of reinforcement. With L_{rein}/H of 0.5 in test WT19, a maximum displacement of 95 mm was observed at the top of the wall and the displacement reduced to 85 mm when L_{rein}/H was increased to 0.7, and it further reduced to 28 mm when the L_{rein}/H was 1.0. Reduction in displacements from L_{rein}/H of 0.5 to 0.7 is marginal. However, displacements for L_{rein}/H of 1.0 are very low, about 33% lesser compared to displacements observed when L_{rein}/H was 0.7, highlighting the importance of maintaining the minimum length of reinforcement in a reinforced retaining wall. In case of geosynthetic-reinforced retaining walls subjected to static loading conditions, a minimum recommended length of reinforcement is about $0.6H$, so that the reinforcement can extend beyond the failure wedge to contribute to the resistance against pullout failure and reduce face deformations (Wu 2019). However, under seismic shaking conditions, the minimum length of reinforcement required is more than $0.7H$ as per the present study because increasing the length of reinforcement beyond $0.7H$ has resulted in

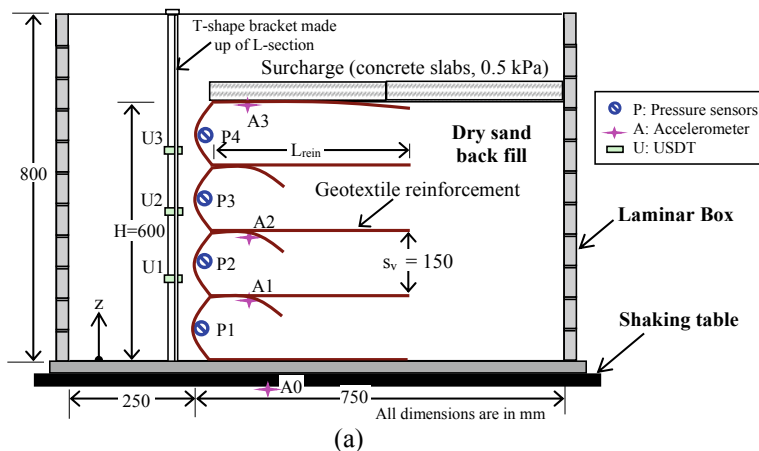


Fig. 15.1 Wrap-faced retaining wall built inside a laminar box. **a** Schematic diagram. **b** Photograph

considerable decrease in lateral deformations. Seismic loads cause additional pullout of reinforcement layers, which needs to be resisted through additional length of reinforcement.

Figure 15.3 shows the effect of reinforcement length on RMSA amplification factors for the tests WT17, WT19 and WT20. Accelerations were amplified by about 1.6 times at the top of the wall for all models, and the difference in acceleration amplifications is not significant for different models. All accelerometers are placed close to the facing, within the reinforced soil zone. Since the relative density of soil is same in all models, soil stiffness and the shear wave velocity within the soil remain same at different elevations. Hence, rate of acceleration amplification

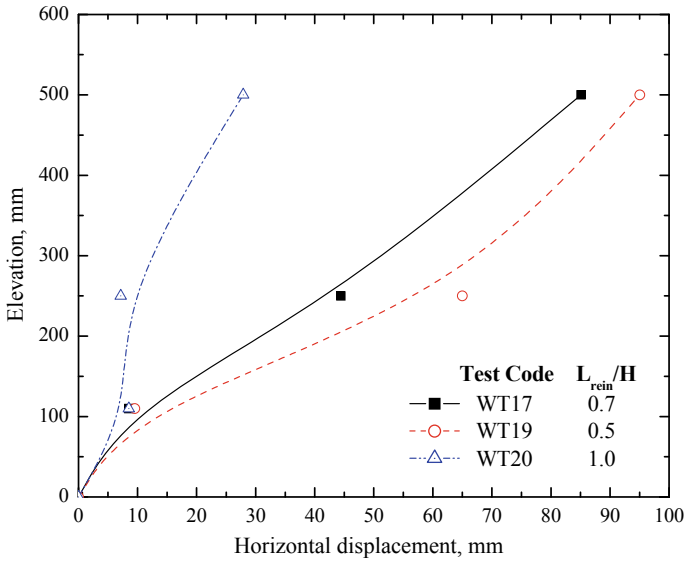


Fig. 15.2 Displacements of wrap-faced walls with change in length of reinforcement

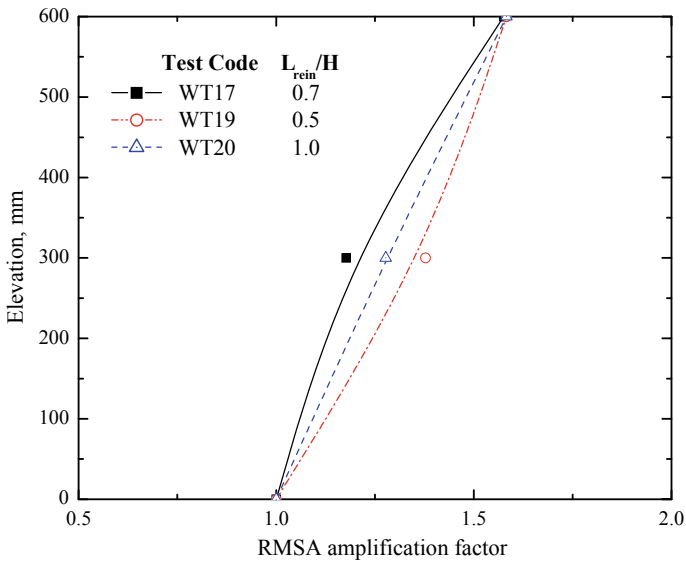


Fig. 15.3 RMSA amplification factors for wrap-faced walls with change in length of reinforcement

does not change with elevation with change in reinforcement length. Similar negligible effect of reinforcement design parameters on amplification factors was reported by El-Emam and Bathurst (2004).

15.3.2 Rigid-Faced Retaining Walls

Rigid-faced retaining walls were constructed to same dimensions as the wrap-faced walls. However, facing in these wall models was created using 12 rectangular hollow steel sections connected through three vertical steel rods running through them, which are rigidly fixed to the base of the laminar box to create a rigid steel panel facing of 600 mm height and 25 mm thickness. Both unreinforced and geogrid reinforced retaining wall models were tested. Biaxial geogrids made of polypropylene with ultimate tensile strength of 26 kN/m at peak strain of 16.5%, and low strain (2%) secant modulus of 219 kN/m were used as reinforcement in these models. Geogrids were run through the steel rods connected with the rigid facing. Dimensional and construction details of rigid faced walls along with the instrumentation are presented in Fig. 15.4.

Length of reinforcement was 420 mm in all reinforced walls. The number of reinforcing geogrid layers was varied in different model tests. Test UT4 represents unreinforced model, while tests RT6, RT7, RT8 and RT9 represent models with 4, 3, 2 and single-layer geogrid models, respectively. Geogrid layers were equally spaced in models. A surcharge pressure of 0.5 kPa is applied over the retaining wall. Shaking table tests were conducted for 20 cycles of sinusoidal dynamic motion of 0.1 g acceleration and 1 Hz frequency.

Figure 15.5 shows the wall deformations for unreinforced and rigid-faced retaining walls at 1 and 2 Hz frequencies. These figures clearly demonstrate the beneficial effects of geosynthetic reinforcement in reducing the deformations of rigid faced walls. Unreinforced retaining wall deformed to a maximum of 1.6 mm, and the deformations were reduced to 0.25 mm with four layers of geogrid reinforcement. Acceleration amplifications were not significant in rigid-faced retaining walls because of the confinement effect created by the rigid wall facing, which imparts additional stiffness to the soil, allowing the shear waves to pass quickly through the soil from bottom to top, thus causing lesser differential accelerations at the bottom and top of the wall. However, difference in acceleration amplifications with increase in the number of reinforcing layers is not significant.

15.3.3 Segmental Retaining Walls

Segmental retaining wall models were built to a length of 0.7 m in the direction of shaking, 0.5 m in the horizontal direction perpendicular to it and 0.6 m height inside the laminar box. The facing for these walls was made using concrete blocks

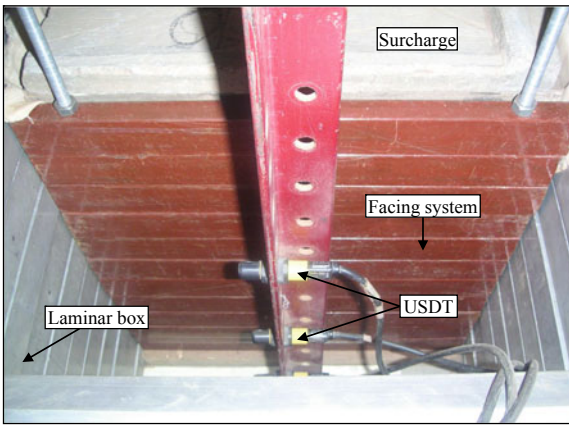
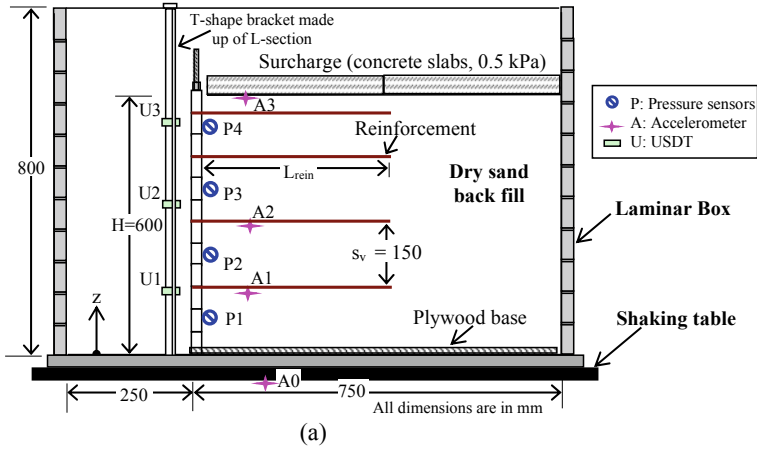


Fig. 15.4 Rigid faced retaining wall built inside a laminar box. **a** Schematic diagram. **b** Photograph

of dimensions 125 mm × 100 mm × 150 mm with an interlocking lip, forming an inward batter of 7.2°. Backfill sand was placed in equal lifts of 150 mm thickness, a layer of geogrid placed at the between two modular facing blocks, as shown in Fig. 15.6. Biaxial geogrids made of polypropylene with ultimate tensile strength of 26 kN/m at peak strain of 16.5% and low strain (2%) secant modulus of 219 kN/m were used as reinforcement in these models. The number of reinforcement layers was 2 and 3 in different tests with equal spacing between the layers. Length of reinforcement was kept as 420 mm in all reinforced walls. A surcharge pressure of 0.5 kPa is applied over the retaining wall. Shaking table tests were conducted for 20 cycles of 0.3 g acceleration at 2 Hz frequency.

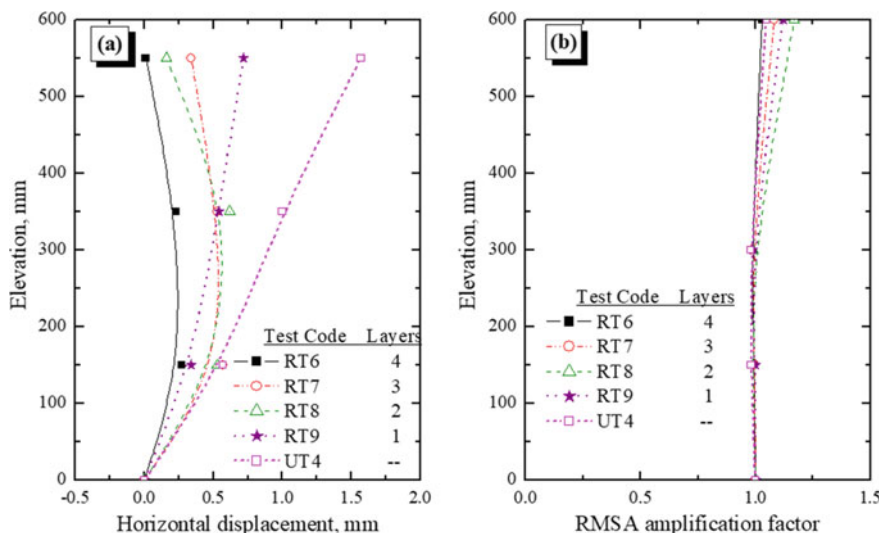
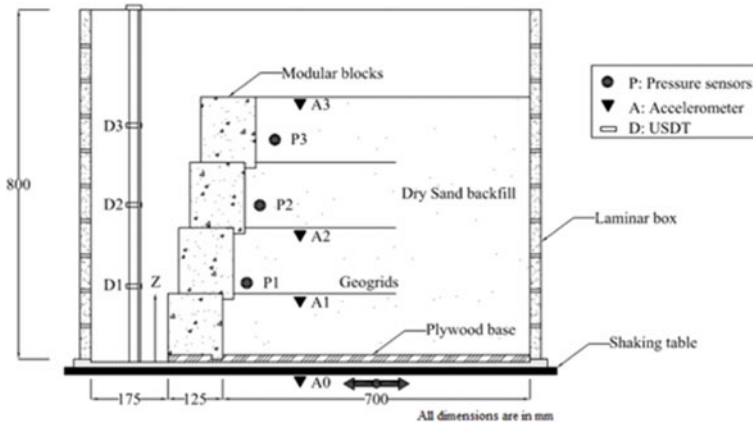


Fig. 15.5 Performance of rigid-faced retaining walls under base shaking conditions. **a** Displacement response. **b** Acceleration amplification response

Figure 15.7 shows the variation of wall deformations and RMSA amplification factors for unreinforced and reinforced modular block walls. Maximum displacement of 6 mm observed in case of unreinforced segmental retaining walls was reduced to less than 1 mm with three layers of geogrid reinforcement. This high reduction in deformations can be related to the increased connectivity between the wall facing and backfill in reinforced walls and additional confinement provided by the reinforcement layers, which restricts the movement of the backfill and thus controls the wall deformations. RMSA amplification factors estimated for the reinforced retaining walls in the present study ranged between 1.1 and 1.3, which is same for unreinforced walls. Appreciable difference is not observed in acceleration amplifications of unreinforced and reinforced segmental retaining walls. Since the stiffness of reinforcement is very low compared with the stiffness of the segmental blocks at the facing and the inward batter of the walls with larger base provides a stable configuration of the wall even without the reinforcement, change in the velocity of wave passing vertically from the base to the top of the wall is not significant with the inclusion of reinforcement.

15.3.4 Geocell Retaining Walls

Geocell retaining walls have backfill retained by the three-dimensional polymeric cells filled with granular fill acting like a facing. In this study, geocell retaining walls of 0.6 m height with and without reinforcement layers in backfill are



(a)



(b)

Fig. 15.6 Segmental retaining wall built inside a laminar box. **a** Schematic diagram. **b** Photograph

constructed inside the laminar box to base dimensions of 0.8 m in the direction of shaking and 0.5 m in the orthogonal direction to shaking in plan. The walls are bettered toward the backfill, with the crest dimensions coming to 0.55 m in the direction of shaking and 0.5 m in the direction perpendicular to it in plan. Backfill was placed using dry pluviation technique, in six layers of 0.1 m height each, which is equal to the height of geocell layer. Geocells were manufactured using polyvinylchloride (PVC) sheets to dimensions of 100 mm × 100 mm × 100 mm, with laminated joints. The PVC sheet has ultimate tensile strength of 0.6 kN/m at a peak strain of 24% and secant modulus of 5 kN/m with seam strength of 0.45 kN/m. Geocell layers were sequentially laid and filled with aggregate of 12 mm average size and compacted to a relative density of 70%. Backfill sand was poured to the height of 0.1 m to the specific relative density before the second layer of geocell is stacked. An offset is maintained to get the retaining wall constructed to

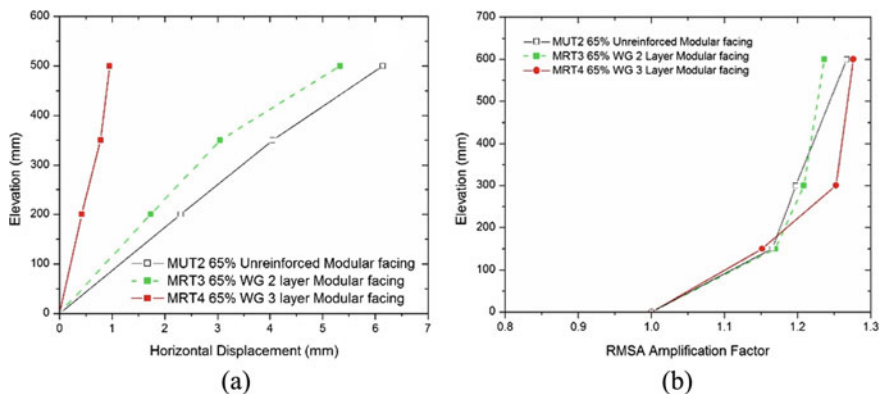


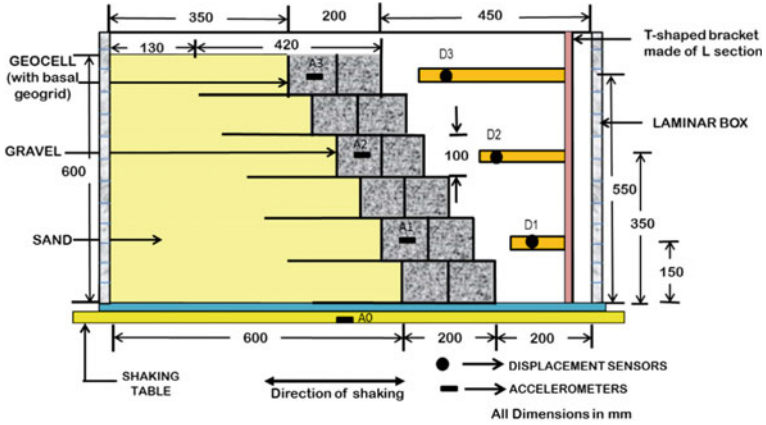
Fig. 15.7 Performance of unreinforced and reinforced segmental retaining walls under base shaking conditions. **a** Displacement response. **b** Acceleration amplification response

with a batter of about 65°. In case of reinforced backfill, a layer of geonet of 0.42 m length with ultimate tensile strength of 11 kN/m is placed between the geocell layers, extending into backfill. Figure 15.8 gives the dimensional details of geocell wall models along with instrumentation.

Geocell retaining walls were subjected to horizontal shaking of 0.3 g and 7 Hz for 20 cycles. Test code S7A3F7 represents the test without geonet in backfill, and the test code S7BA3F7 represents the test with geonet layers in backfill. Difference in facing deformations and acceleration amplifications of the walls without geonet reinforcement in backfill and walls with geonet reinforcement are compared in Fig. 15.9.

Results showed that reinforcement in backfill resulted in about 60% reduction in wall deformations. When the geocell walls have no reinforcement in backfill, lateral pressures on the wall facing are more, resulting in more wall deformations. Layers of geonet provided extra confinement effect to the backfill because of which the backfill exerts lesser lateral pressures on wall facing, causing the walls move relatively lesser during shaking. Also, the internal movement of backfill is restricted due to the separation effect of geonet layers, which resulted in better friction mobilization during shaking and hence acted against the movement of wall.

Considerable reduction in RMSA amplification factors was observed with the geonet reinforcement. The reduction was from a value of 2.2 to 1.5 at the top of the wall where the amplifications were maximum. These huge reductions in RMSA amplification factors can be attributed to the overall increase in wall stiffness due to the inclusion of geonets. In case of models without a basal geonet, the connection between the wall facing and the backfill is established only through the stepped geometry of the geocell walls. Hence, the wall components (facing and backfill) might lose connection during seismic shaking, which results in higher deformations and amplification factors. In case of walls geonet, since the geonet is connecting the wall facing with the backfill more effectively, the wall moves as a whole, and



(a)



(b)

Fig. 15.8 Geocell retaining wall built inside a laminar box. **a** Schematic diagram. **b** Photograph

hence, even stronger ground shaking cannot separate them, and hence, the deformations and acceleration amplifications are lesser. The geonet used in this study has very low tensile strength, and in prototype models, it matches with the tensile strength of commercial geosynthetics with higher tensile strength.

15.4 Conclusions

Through shaking table studies on models of wrap-faced, rigid-faced, segmental and geocell retaining walls, it is demonstrated that geosynthetic reinforcement provides appreciable benefits for the seismic performance of these walls. These benefits are highly significant in reducing the deformations of the walls. Even with weaker geosynthetic reinforcement, deformations were reduced by a minimum of 30% and

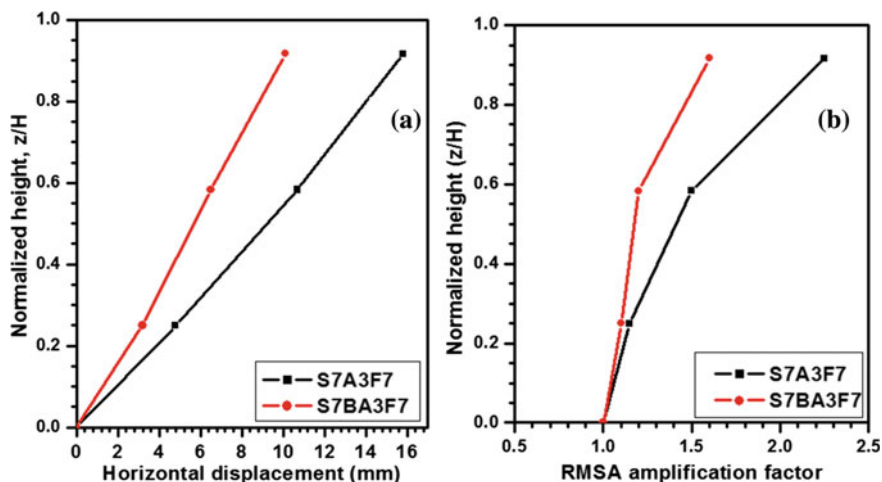


Fig. 15.9 Performance of geocell walls with and without backfill reinforcement

in some cases more than 80%. Reinforcement was found to be an effective means to confine the backfill soil and to establish stable connectivity between wall facing and the backfill soil so that the lateral pressures on the facing from backfill can be effectively controlled. However, effect of reinforcement on acceleration amplifications in retaining walls is not significant because the improvement in stiffness within the model scale walls is not good enough to alter the velocity of shear waves traveling from wall base to the top of the wall. Studies reported in this paper are carried out using 1-g model tests, and hence, the results are subjected to scaling effects and stress discrepancies between the models and prototype walls. However, qualitatively, the benefits of using geosynthetic reinforcement in retaining walls for their enhanced seismic performance are clearly established from this study.

References

- Bathurst RJ, Hatami K (1998) Seismic response analysis of a geosynthetic-reinforced soil retaining wall. *Geosynth Int* 5(1–2):127–166
- Chen HT, Hung WY, Chang CC, Chen YJ, Lee CJ (2007) Centrifuge modeling test of a geotextile-reinforced wall with a very wet clayey backfill. *Geotext Geomembr* 25(6):346–359
- Clough RW, Pirtz D (1956) Earthquake resistance of rockfill dams. *J Soil Mech Found Div* 82 (2):1–26
- Coe CJ, Prevost JH, Scanlan RH (1985) Dynamic stress wave reflection/attenuation: earthquake simulation in centrifuge soil models. *Earthquake Eng Soil Dyn* 13:109–128
- El-Emam M, Bathurst RJ (2004) Experimental design, instrumentation and interpretation of reinforced soil wall response using a shaking table. *Int J Phys Model Geotech* 4:13–32
- El-Emam MM, Bathurst RJ (2007) Influence of reinforcement parameters on the seismic response of reduced-scale reinforced soil retaining walls. *Geotext Geomembr* 25(1):33–49

- Iai S (1989) Similitude for shaking table tests on soil-structure fluid model in 1-g gravitational field. *Soils Found* 29(1):105–118
- Koerner RM (2012) *Designing with geosynthetics*, 4th edn. Prentice Hall Inc., New Jersey
- Krishna AM, Latha GM (2007) Seismic response of wrap-faced reinforced soil retaining wall models using shaking table tests. *Geosynth Int* 14(6):355–364
- Krishna AM, Latha GM (2009) Container boundary effects in shaking table tests on reinforced soil wall models. *Int J Phys Model Geotech* 9(4):1–14
- Latha GM, Santhanakumar P (2015) Seismic response of reduced-scale modular block and rigid faced reinforced walls through shaking table tests. *Geotext Geomembr* 43(4):307–316
- Leshchinsky D, Ling HI, Wang J-P, Rosen A, Mohri Y (2009) Equivalent seismic coefficient in geocell retention systems. *Geotext Geomembr* 27(1):9–18
- Li AL, Rowe RK (2008) Effects of viscous behaviour of geosynthetic reinforcement and foundation soils on the performance of reinforced embankments. *Geotext Geomembr* 26: 317–334
- Ling HI, Leshchinsky D, Wang J, Mohri Y, Rosen A (2009) Seismic response of geocell retaining walls, experimental studies. *J Geotech Geo-Environ Eng ASCE* 135(4):515–524
- Lo Grasso AS, Maugeri M, Recalcati P (2005) Seismic behaviour of geosynthetic-reinforced slopes with overload by shaking table tests. In: *Slopes and retaining structures under seismic and static conditions*. ASCE Geotechnical Special Publication No. 140, CDROM
- Panah AK, Yazdi M, Ghalandarzadeh A (2015) Shaking table tests on soil retaining walls reinforced by polymeric strips. *Geotext Geomembr* 43:148–161
- Perez A, Holtz RD (2004) Seismic response of reinforced steep soil slopes: results of a shaking table study. In: *Geotechnical engineering for transportation projects*, vol 126. ASCE Geotechnical Special Publication, pp 1664–1672
- Sakaguchi M (1996) A study of the seismic behavior of geosynthetic reinforced walls in Japan. *Geosynth Int* 3(1):13–30
- Sugimoto M, Ogawa S, Moriyama M (1994) Dynamic characteristics of reinforced embankments with steep slope by shaking model tests. In: *Recent case histories of permanent geosynthetic-reinforced soil walls*, Seiken symposium, Tokyo, Japan, pp 271–275
- Telekes G, Sugimoto M, Agawa S (1994) Shaking table tests on reinforced embankment models. In: *Proceedings of 13th international conference on soil mechanics and foundation engineering*, New Delhi, India, vol 2, pp 649–654
- Turan A, Hinchberger SD, El Naggar H (2009) Design and commissioning of a laminar soil container for use on small shaking tables. *Soil Dyn Earthq Eng* 29:404–414
- Wang L, Chen G, Chen S (2015) Experimental study on seismic response of geogrid reinforced rigid retaining walls with saturated backfill sand. *Geotext Geomembr* 43(1):35–45
- Wood DM, Crewe A, Taylor C (2002) Shaking table testing of geotechnical models. *Int J Phys Model Geotech* 1:1–13
- Wu JTH (2019) *Geosynthetic reinforced soil (GRS) walls*. Wiley, Hoboken, NJ